R. & M. No. 3135
(20,299)
A.R.C. Technical Report

MINISTRY OF AVIATION

AERONAUTICAL RESEARCH COUNCIL
REPORTS AND MEMORANDA

The Properties of a Thin Conically Cambered Wing according to Slender-Body Theory

By J. H. B. Smith

LONDON: HER MAJESTY'S STATIONERY OFFICE
1960
PRICE 9*s.* 6*d.* NET

The Properties of a Thin Conically Cambered Wing according to Slender-Body Theory

By J. H. B. Smith

Communicated by the Director-General of Scientific Research (Air)
Ministry of Supply

*Reports and Memoranda No. 3135**
March, 1958

Summary. Slender-body theory is used to calculate the lift and drag forces acting on a thin slender delta wing cambered to form part of the surface of a circular cone, in the type of flow in which separation is from the trailing edge only. The boundary condition satisfied by the flow on the wing surface is applied there, instead of on a nearby plane as is usual in linearized theory. This has relatively little effect on the overall forces on a wing at a given incidence. However, a large discrepancy arises between the overall forces at the incidence for which the singularity in the pressure at the leading edge vanishes, as calculated by the present and by the usual linearized theory. This is particularly important, since it is at this incidence that the type of flow treated is expected to be realized in a physical fluid. The lift-dependent drag factor found is below the usual linearized-theory value for this type of wing at the incidence of no leading-edge singularity; and, for large lift, is below unity, which is the minimum for a trailing vortex sheet which is effectively flat.

1. *Introduction.* The partial differential equations which govern the motion of an inviscid fluid are non-linear. To the second order in the perturbations of a uniform stream, the flow is irrotational and a velocity potential exists and satisfies a non-linear second-order equation. For Mach numbers which are neither too high nor too near unity, this equation can be linearized, *i.e.*, the terms in it involving products of derivatives of the perturbation potential can be omitted. The boundary condition to be satisfied in the case of steady, attached† flow past a solid body is the vanishing of the normal derivative of the potential on the surface of the body. The solution of the linearized equation with this exact boundary condition is still difficult, so it is usual to apply the boundary condition on a geometrically simple surface (*e.g.*, a plane, circular cylinder or body of revolution), which is close to the actual surface of the body. For brevity, and the purpose of the present paper, this process will be referred to as 'linearizing the boundary conditions' (clearly this can be done in different ways, but we are not concerned with distinguishing between them). Such a geometrically simple surface, parallel to the undisturbed stream, can be found for most aircraft components.

* R.A.E. Report Aero. 2602, received 10th July, 1958.

† We use 'attached flow' to mean (inviscid) flow with separation from trailing edges only or flow which has vorticity only in the wake.

Since the justification for using the linearized differential equation is the smallness of the perturbations, it can be held that no additional assumption is made in using linearized boundary conditions. Indeed, there is no *a priori* estimation of the errors introduced in the two linearization processes which shows them to be of different orders. Thus it is not claimed on mathematical grounds that the solution of the linearized equation with exact boundary conditions is closer to the solution of the exact equation with the same boundary conditions, either in general, or in any particular case. On the other hand, it is certainly true that if the use of the exact boundary conditions produces results which differ unacceptably from those obtained using the linearized boundary condition, the latter cannot be relied on (they could, through compensating errors for instance, be correct; but they would not be trustworthy). If the results from the exact and linearized boundary conditions agree closely, confidence in the linearization of the differential equation may be increased, since in some sense thé perturbations are small. If they differ, and no better treatment is available, we may be inclined on intuitive grounds to favour the treatment using the exact condition*. Furthermore, in the particular solution obtained in the present paper, it is easily seen that, for the ranges of the parameters considered, the perturbations of the stream are of higher order than the discrepancies introduced when the boundary conditions are linearized. This point is taken up again in Section 3.

The only solutions using exact boundary conditions for the flow round a given wing are effectively two-dimensional. Many solutions for thick, cambered aerofoils in plane flow exist. In supersonic conical-flow theory the elliptic cone at zero incidence and the flat delta at incidence have been studied[1] using the exact boundary conditions and the linearized equation. Further attempts[2, 3] at similar problems have been made using the exact equation and exact conditions. In slender-body theory, bodies of elliptic cross-section have been studied[4, 5, 6] and there are also solutions[7, 8] for combinations of plane wings and bodies of revolution at incidence. However, no solutions for cambered, three-dimensional wings are known.

It has recently become clear that there is a need to be able to assess the applicability of the linearized equation and, more particularly, the linearized boundary conditions, to the flow past slender, cambered wings. Recent work[9, 10, 11] on the design of slender wings to maintain attached flow has suggested that mean surfaces with steep slopes near the leading edge may be necessary, and it is not certain that the theory using the linearized equation and boundary condition which satisfactorily predicts the properties of flat or slightly warped wings will be adequate to deal with them. The perturbation velocities predicted by the linearized equation for the flow past a wing warped to maintain attached flow are finite everywhere; in contrast to those predicted for a lifting flat plate, for instance. Thus the linearization of the differential equation seems to be at least as well justified *a posteriori* for the warped wing as in many other cases where it is accepted. Therefore, in the present paper the aerodynamic characteristics of a slender delta wing, in the form of a sector of the surface of a circular cone, are studied by slender-body theory, *i.e.*, making use of the exact boundary condition.

---

* The situation here is parallel to that occurring in the calculation of pressures in supersonic linearized theory. The quadratic terms in Bernoulli's equation for the pressure coefficient are of the same relative order, mathematically, as the terms omitted in linearizing the differential equation. If, arithmetically, they materially modify the pressure coefficient, only the breakdown of the theory can strictly be deduced, though intuitively we may accept the modified result.

The properties of such slender configurations without thickness are given by slender-body theory in terms of the solution of a two-dimensional harmonic problem in the cross-flow plane, in a form independent of Mach number. The validity of this for subsonic and low supersonic speeds is well known[7] and has recently been established[12] for transonic speeds also. The present treatment proceeds by transforming conformally the cross-flow plane exterior to the circular arc in which the wing meets it into the region of the plane exterior to a straight slit. The complex potential corresponding to the distribution of normal velocity on the slit, as prescribed by the condition of no velocity normal to the three-dimensional surface, is then constructed. This is done by considering a continuation of the normal velocity and eliminating its singularities in a third plane where the slit is transformed into a circle.

This potential is a complicated function, so, instead of calculating the perturbation velocities and pressures on the wing, the lift and drag are evaluated in a plane behind the wing. These are given by expressions involving the incidence and a parameter representing the camber of the wing. The first term of an expansion in powers of the latter is the solution of the problem with the linearized boundary condition. The expressions depart further from this as the camber increases, *i.e.*, as the wing includes a greater proportion of the surface of the cone.

It is known that the physical flow past a sharp-edged slender wing with a conical mean surface, such as that considered here, separates at the leading edge except near one particular incidence. This separation is associated with the singularity of the attached-flow solution at such an edge and is believed not to occur at the incidence for which this singularity vanishes. The type of flow which is treated in this paper, however, has separation from the trailing edge only, so that the present theory can only be expected to apply to real flows at the incidence on each wing for which it predicts finite velocities everywhere. Numerical results are therefore presented and discussed in more detail for each wing of the family at this incidence.

2. *Solution of the Problem.* 2.1. *Boundary Values.* We consider a slender delta wing without thickness, warped to form part of a circular cone. We use right-handed rectangular Cartesian axes arranged as in Fig. 1, with the origin, O, at the wing (and cone) apex, Oxy the plane of the leading edges, Oy to starboard and Ox downstream. The leading edges are the lines $|y| = s = Kx$ and the warp is such that the section of the wing by the cross-flow plane $x = \text{const}$ is a circular arc rising a distance βs above the plane Oxy of the leading edges. This plane is at an incidence α to the undisturbed stream of velocity U, which is resolved into components $U\cos\alpha$ along Ox and $U\sin\alpha$ along Oz. These two components are treated separately in the present analysis, so that we seek a function ϕ such that the velocity potential is $Ux\cos\alpha + \phi$. Thus $\phi \sim Uz\sin\alpha$ at a large distance from the wing.

Introducing the angle δ by $\beta = \tan\delta\ (O \leqslant \delta \leqslant \pi/4)$, we find the geometrical relations shown in Fig. 2, in the complex plane $Z = y + iz$. The equation to the cone is seen to be

$$S \equiv y^2 + (z + \cot 2\delta\, Kx)^2 - \operatorname{cosec}^2 2\delta\, K^2x^2 = 0\,. \tag{1}$$

Now, provided the wing is slender, i.e., $K^2 \ll 1$, the velocity normal to the contour in the cross-flow plane due to the component $U\cos\alpha$ is given by:

$$\frac{\partial\phi}{\partial n} = \frac{U\cos\alpha\,(\partial S/\partial x)}{\left\{\left(\frac{\partial S}{\partial y}\right)^2 + \left(\frac{\partial S}{\partial z}\right)^2\right\}^{1/2}}, \tag{2}$$

which is equivalent to requiring the wing to lie in a stream surface in three dimensions. Taking n to be the upward, outward normal, equations (1) and (2) show that

$$\frac{\partial \phi}{\partial n} = KU \cos \alpha \ \sin 2\delta \left(1 - \frac{z}{s} \cot 2\delta\right).$$

Introducing an angular co-ordinate θ on the arc (*see* Fig. 2) so that, on the arc,

$$y = s \operatorname{cosec} 2\delta \ \sin 2\theta, \qquad z = -s \cot 2\delta + s \operatorname{cosec} 2\delta \ \cos 2\theta :$$

we find:

$$\frac{\partial \phi}{\partial n} = KU \cos \alpha \ \operatorname{cosec} 2\delta (1 - \cos 2\delta \ \cos 2\theta), \tag{3}$$

where

$$Z = s \operatorname{cosec} 2\delta (\sin 2\theta - i \cos 2\delta + i \cos 2\theta). \tag{4}$$

We now consider the transformation (*see* Fig. 2), which takes the plane slit along the circular arc into the plane slit along the line: $\mathscr{I}\{\zeta\} = 0, -s \leqslant \mathscr{R}\{\zeta\} \leqslant s$; and the point at infinity into a finite point; *i.e.*,

$$\frac{\zeta}{s} = \frac{Z - i\beta s}{s - i\beta Z}, \qquad \frac{Z}{s} = \frac{\zeta + i\beta s}{s + i\beta \zeta}, \qquad \frac{dZ}{d\zeta} = \frac{s^2(1 + \beta^2)}{(s + i\beta\zeta)^2}. \tag{5}$$

On the slits the point θ in the Z plane becomes the point $\zeta = s \cos \psi$, where

$$\cos \psi = \frac{\tan \theta}{\tan \delta} = \frac{\tan \theta}{\beta} \tag{6}$$

by equations (4) and (5). Similarly the modulus of the transformation $\left|\frac{dZ}{d\zeta}\right|$ is given on the slit by:

$$\left|\frac{dZ}{d\zeta}\right| = \cos^2 \theta (1 + \beta^2) = \frac{1 + \beta^2}{1 + \beta^2 \cos^2 \psi}. \tag{7}$$

Thus the required normal velocity on the slit in the ζ plane is given by:

$$\left.\frac{\partial \phi}{\partial n}\right|_{\zeta} = \left.\frac{\partial \phi}{\partial n}\right|_{z} \left|\frac{dZ}{d\zeta}\right| = KU \cos \alpha \frac{\beta(1 + \beta^2)(1 + \cos^2 \psi)}{(1 + \beta^2 \cos^2 \psi)^2} \tag{8}$$

at $\zeta = s \cos \psi$, using equations (3), (6) and (7).

2.2. *Complex Potential.* We now construct a complex potential W in the cross-flow plane so that the complete potential is $Ux \cos \alpha + \mathscr{R}\{W\}$. W must then behave like $-iUZ \sin \alpha$ for large Z and the real part of its normal derivative must take the values (3) or (8) on the contour. It is allowed to have branch points at the leading edges, but must otherwise be non-singular in the finite part of the Z plane. We first find a complex potential which produces the correct normal derivative on the contour and then modify it by adding sources, sinks and doublets so as to remove its unwanted singularities without changing the normal derivative on the contour.

The function

$$KU \cos \alpha \frac{\beta(1 + \beta^2)s^2(s^2 + \zeta^2)}{(s^2 + \beta^2\zeta^2)^2} \tag{9}$$

is an obvious continuation of the right-hand side of (8), taking the same values on the slit $\mathscr{I}(\zeta) = 0$, $-s \leqslant \mathscr{R}(\zeta) \leqslant s$. Now (9) is minus the imaginary part of the derivative with respect to ζ of

$$\frac{KUs\cos\alpha(1+\beta^2)}{4\beta^2}\left\{(1+\beta^2)\log\frac{\beta\zeta+is}{\beta\zeta-is}+is(1-\beta^2)\left(\frac{1}{\beta\zeta-is}+\frac{1}{\beta\zeta+is}\right)\right\}. \tag{10}$$

Thus (10) is a complex potential with the correct normal derivative on the contour.

To make clear the adjustment of the singularities, we introduce the Z^* plane in which the wing slit becomes the unit circle. Then

$$Z^* = \frac{\zeta}{s} + \sqrt{\left(\frac{\zeta^2}{s^2}-1\right)}, \qquad \frac{\zeta}{s} = \frac{1}{2}\left(Z^* + \frac{1}{Z^*}\right) \tag{11}$$

and (10) becomes

$$\begin{aligned}\frac{KUs\cos\alpha(1+\beta^2)}{4\beta^2}\Bigg[&(1+\beta^2)\log\frac{\beta Z^*+i\{1+\sqrt{(1+\beta^2)}\}}{\beta Z^*-i\{1+\sqrt{(1+\beta^2)}\}}\frac{\beta Z^*-i\{-1+\sqrt{(1+\beta^2)}\}}{\beta Z^*+i\{-1+\sqrt{(1+\beta^2)}\}}+\\&+\frac{i(1-\beta^2)\beta^2}{\sqrt{(1+\beta^2)}}\left\{\frac{1}{1+\sqrt{(1+\beta^2)}}\left(\frac{1}{\beta Z^*+i\{-1+\sqrt{(1+\beta^2)}\}}+\frac{1}{\beta Z^*-i\{-1+\sqrt{(1+\beta^2)}\}}\right)\right.\\&\left.+\frac{1}{-1+\sqrt{(1+\beta^2)}}\left(\frac{1}{\beta Z^*-i\{1+\sqrt{(1+\beta^2)}\}}+\frac{1}{\beta Z^*+i\{1+\sqrt{(1+\beta^2)}\}}\right)\right\}\Bigg].\end{aligned} \tag{12}$$

This is the complex potential of two sources, two sinks and four doublets, of which one source, one sink and two doublets lie outside $|Z^*| = 1$ and are therefore to be removed. This is done without upsetting the normal velocity on the circle by introducing cancelling singularities outside $|Z^*| = 1$ with their image systems inside the circle. The source and sink at the centre of the circle cancel and the other singularities introduced inside the circle double the strengths of those already there. In addition, we must introduce a doublet at the point $Z^* = i\{1+\sqrt{(1+\beta^2)}\}/\beta$, corresponding to the point at infinity in the Z plane, with the strength appropriate to a velocity $dW/dZ \sim -iU\sin\alpha$ as Z tends to infinity; together with an image doublet in the unit circle. The result of these modifications to (12) is the complex potential:

$$\begin{aligned}W = \frac{KUs\cos\alpha(1+\beta^2)}{2\beta^2}&\left\{(1+\beta^2)\log\frac{\beta Z^*-i\{-1+\sqrt{(1+\beta^2)}\}}{\beta Z^*+i\{-1+\sqrt{(1+\beta^2)}\}}+\right.\\&\left.+\frac{i(1-\beta^2)\beta^2}{\sqrt{(1+\beta^2)}\{1+\sqrt{(1+\beta^2)}\}}\left(\frac{1}{\beta Z^*+i\{-1+\sqrt{(1+\beta^2)}\}}+\frac{1}{\beta Z^*-i\{-1+\sqrt{(1+\beta^2)}\}}\right)\right\}+\\&+\frac{iUs\sin\alpha\sqrt{(1+\beta^2)}}{\beta}\left(\frac{-1+\sqrt{(1+\beta^2)}}{\beta Z^*-i\{-1+\sqrt{(1+\beta^2)}\}}-\frac{1+\sqrt{(1+\beta^2)}}{\beta Z^*-i\{1+\sqrt{(1+\beta^2)}\}}\right).\end{aligned} \tag{13}$$

This can be re-written in terms of ζ, using (11):

$$\begin{aligned}W = &\frac{KUs\cos\alpha(1+\beta^2)^2}{4\beta^2}\log\frac{s-i\beta\zeta\, s\sqrt{(1+\beta^2)}+i\beta\sqrt{(\zeta^2-s^2)}}{s+i\beta\zeta\, s\sqrt{(1+\beta^2)}-i\beta\sqrt{(\zeta^2-s^2)}}\\&+\frac{iKUs^2\cos\alpha(1-\beta^2)\sqrt{(1+\beta^2)}}{2\beta\{\sqrt{(1+\beta^2)}\zeta+\sqrt{(\zeta^2-s^2)}\}}-\frac{iUs^2\sin\alpha\sqrt{(1+\beta^2)}}{\beta\{\beta\sqrt{(\zeta^2-s^2)}-is\sqrt{(1+\beta^2)}\}},\end{aligned} \tag{14}$$

and so

$$\frac{dW}{d\zeta} = \frac{iKUs^2 \cos\alpha(1+\beta^2)^2\{\zeta\sqrt{(1+\beta^2)} - \sqrt{(\zeta^2 - s^2)}\}}{2\beta(s^2+\beta^2\zeta^2)\sqrt{(\zeta^2-s^2)}} +$$

$$- \frac{iKUs^2\cos\alpha(1-\beta^2)\sqrt{(1+\beta^2)}\{\zeta\sqrt{(1+\beta^2)} - \sqrt{(\zeta^2-s^2)}\}^2\{\zeta + \sqrt{(1+\beta^2)}\sqrt{(\zeta^2-s^2)}\}}{2\beta(s^2+\beta^2\zeta^2)^2\sqrt{(\zeta^2-s^2)}}$$

$$+ \frac{iUs^2\sin\alpha\sqrt{(1+\beta^2)}\zeta\{\beta\sqrt{(\zeta^2-s^2)} + is\sqrt{(1+\beta^2)}\}^2}{(s^2+\beta^2\zeta^2)^2\sqrt{(\zeta^2-s^2)}}. \tag{15}$$

At this point it is convenient to mention the relationship of the present problem to others in aerodynamic theory which involve circular arcs, *e.g.*, the (part) annular wing of small chord and the two-dimensional circular-arc profile. In each case we require a solution of Laplace's equation with a prescribed behaviour at infinity and, in contrast to the present case, zero normal derivative on the circular arc. For the annular wing there is no total circulation about the section of the wake in the Trefftz plane; and for the two-dimensional profile, the circulation is determined by the Kutta-Jowkowski condition. The same transformation can be used in these problems, but the expressions found are much simpler. For instance, for the part annular wing of small chord, the lift and drag are given by the present theory with K zero and α twice the geometrical incidence of the wing.

2.3. *Pressure and Load Distribution.* The pressure coefficient, to the same order as the linearized equation for the potential, is given, for slender configurations, by

$$C_p = -\frac{2}{U}\frac{\partial\phi}{\partial x} - \frac{1}{U^2}\left\{\left(\frac{\partial\phi}{\partial y}\right)^2 + \left(\frac{\partial\phi}{\partial z}\right)^2\right\} + \sin^2\alpha, \tag{16}$$

where $\phi = \phi(x, y, z) = \mathscr{R}\{W\}$. The differentiation with respect to x is for constant y and z, i.e., constant Z, so that:

$$\frac{\partial\phi}{\partial x} = \mathscr{R}\left\{\left.\frac{\partial W}{\partial x}\right|_{Z\text{ const}}\right\} = \mathscr{R}\left\{\left.\frac{\partial W}{\partial x}\right|_{\zeta\text{ const}} + \left.\frac{\partial W}{\partial\zeta}\right|_{x\text{ const}} \times \left.\frac{\partial\zeta}{\partial x}\right|_{Z\text{ const}}\right\}. \tag{17}$$

$\partial\phi/\partial z$ is continuous on the slit but $\partial\phi/\partial y$ is not antisymmetric in this solution, so that the non-dimensional load distribution is given by

$$l = -\Delta\{C_p\} = \Delta\left\{\frac{2}{U}\frac{\partial\phi}{\partial x} + \frac{1}{U^2}\left(\frac{\partial\phi}{\partial y}\right)^2\right\}_{\text{on the wing}}. \tag{18}$$

Equations (16), (17), (18) make the calculation of the pressure and load from (14) a straightforward, though complicated, procedure. The expressions are too cumbersome to be worth publishing. Fortunately we can obtain the overall forces more simply, after we have restricted the range of incidence required.

2.4. *Overall Forces.* As explained in the introduction, the flow model studied here is only expected to be adequate for incidences near that at which the leading-edge singularity in load and

velocity vanishes. We denote this incidence by α_0. It is sufficient* to require that the cross-flow velocity be non-singular at $Z = \pm s$, or that $dW/d\zeta$ be non-singular at $\zeta = \pm s$. Referring to equation (15), we see that the coefficient of $(\zeta^2 - s^2)^{-1/2}$ in $dW/d\zeta$ vanishes at $\zeta = \pm s$ if and only if

$$\tan \alpha = \tfrac{1}{2}\beta(3 + \beta^2)K .$$

Now $K^2 \ll 1$, $\beta = O(1)$ and so

$$\alpha^2 \ll 1 , \tag{19}$$

$$\alpha_0/K = \tfrac{1}{2}\beta(3 + \beta^2) \tag{20}$$

near, and at, respectively, the incidence for which the coefficient of the singularity vanishes.

Having verified that the incidences we consider are small, we proceed to calculate the overall forces. Consider a control surface consisting of a streamwise cylinder surrounding the wing terminated by a plane ahead of the wing and a plane through the trailing edge, both normal to the stream. Then, for a slender configuration without thickness, the expressions for the lift and drag reduce to integrals over the plane through the trailing edge. Since we are considering a more exact treatment than usual, it is appropriate to distinguish between the plane normal to the free stream and the plane x = constant. Consider new co-ordinates $Ox'y'z'$ rotated through α about Oy (*see* Fig. 3). Then

$$\left.\begin{aligned} x &= x' \cos\alpha - z' \sin\alpha & x' &= x \cos\alpha + z \sin\alpha \\ z &= x' \sin\alpha + z' \cos\alpha & z' &= -x \sin\alpha + x \cos\alpha \\ y &= y' & y' &= y \end{aligned}\right\} . \tag{21}$$

The lift (normal to the free stream) is given by the integral:

$$L = -\rho U \int \left[Ux \cos\alpha + \mathscr{R}\{W\} \right]_{\text{upper}}^{\text{lower}} dy' ,$$

where the integral is taken along the wake, in the plane x' = const.

Now (*see* Fig. 3) the values of W on the wake at the same value of $y' = y$ in planes x' = const and x = const through the trailing edge are the same to the order of α^2 (*i.e.*, the order of K^2 for the values of α considered). $Ux \cos\alpha$ and $\mathscr{I}\{W\}$ are continuous functions across the wake and

$$\mathscr{R}\{W\, dZ\} = \mathscr{R}\{W\}\, dy - \mathscr{I}\{W\}\, dz .$$

Thus

$$L = -\rho U\, \mathscr{R}\left\{ \int_C W\, dZ \right\} ,$$

where C is the contour just containing the wake. Since W is analytic outside the wake, this contour can be replaced by any other contour containing the wake, for instance, a large circle. Thus if, for large Z,

$$W = a_1 Z + a_0 + a_{-1} Z^{-1} + \ldots ,$$

---

* For a conical field, this follows from the relation

$$\frac{\partial \phi}{\partial x} = \frac{\phi}{x} - \frac{yv + zw}{x} + \text{a function of } x.$$

In general, it follows by considering the continuity of the bound vortices.

we have

$$L = 2\pi\rho U \, \mathcal{I}\{a_{-1}\} .$$

An expansion of (14) for large Z shows

$$a_{-1} = \tfrac{1}{4}iUs^2 \sin\alpha(2 + \beta^2) - \tfrac{1}{8}iUs^2K \cos\alpha(5 + 3\beta^2)\beta$$

and so

$$L = \pi\rho U^2 s^2 \left\{\alpha\left(1 + \frac{\beta^2}{2}\right) - \beta K \frac{5}{4}\left(1 + \frac{3}{5}\beta^2\right)\right\} .$$

Thus

$$\frac{C_L}{K^2} = 2\pi\left\{\frac{\alpha}{K}\left(1 + \frac{\beta^2}{2}\right) - \frac{5}{4}\beta\left(1 + \frac{3}{5}\beta^2\right)\right\} . \tag{22}$$

based on the projected area of the wing, $S_p = s^2/K$.

The drag (in the stream direction) is given by the energy integral:

$$D = \tfrac{1}{2}\rho \int\int (w'^2 + v'^2)\, dy'\, dz' ,$$

where the integral extends over the plane $x' = \text{const}$ slit along the wake, and w' and v' are the upwash and sidewash in this plane. Transforming the double integral by Green's Theorem for the plane, we have:

$$D = \tfrac{1}{2}\rho \int_{C'} (Ux \cos\alpha + \mathcal{R}\{W\}) v_n' \, d\sigma' ,$$

where v_n' is the velocity along the inward normal to the slit and σ' is the arc length in the plane $x' = \text{const}$ and C' just surrounds the wake. Now $Ux \cos\alpha$ is continuous across the wake and v_n' is equal in magnitude and opposite in sign on the upper and lower surfaces. Further, the values of W in the planes $x' = \text{const}$ and $x = \text{const}$ agree to order α^2. To the same order, v_n' is given by

$$\pm v_n' = -\frac{\partial\phi}{\partial n} + \alpha U \cos 2\theta$$

on the upper and lower surface, where $\partial\phi/\partial n$ is given by (3). Thus we have

$$D = \tfrac{1}{2}\rho \int_{-\delta}^{\delta} \Big[\mathcal{R}\{W\}\Big]_{\text{lower}}^{\text{upper}} \Big(\alpha U \cos 2\theta - KU \operatorname{cosec} 2\delta\,(1 - \cos 2\delta \cos 2\theta)\Big) \times s \operatorname{cosec} 2\delta \, 2d\theta . \tag{23}$$

From (14)

$$\Big[\mathcal{R}\{W\}\Big]_{\text{lower}}^{\text{upper}} = + \frac{\alpha Us \cot\delta}{1 - \sin\delta \sin\psi} - \frac{\alpha Us \cot\delta}{1 + \sin\delta \sin\psi} + KUs \operatorname{cosec}^2 2\delta \left(2 \log \frac{1 - \sin\delta \sin\psi}{1 + \sin\delta \sin\psi} + \frac{\sin 4\delta \cos\delta \sin\psi}{1 - \sin^2\delta \sin^2\psi}\right) . \tag{24}$$

Thus, substituting from (6) and (24) in (23), we find, for the coefficient based on the projected area of the wing,

$$\frac{C_D}{K^3} = \frac{D}{\frac{1}{2}\rho U^2 K^2 s^2} =$$

$$2\int_0^{\pi/2} \left\{ \frac{2\cos\delta \sin\psi}{1-\sin^2\delta \sin^2\psi} \frac{\alpha}{K} + 2\,\mathrm{cosec}^2 2\delta \log \frac{1-\sin\delta \sin\psi}{1+\sin\delta \sin\psi} + \frac{\mathrm{cosec}\,\delta \cos 2\delta \sin\psi}{1-\sin^2\delta \sin^2\psi} \right\} \times$$

$$\left\{ \frac{\alpha}{K} \frac{1-\beta^2\cos^2\psi}{1+\beta^2\cos^2\psi} - \frac{\beta(1+\cos^2\psi)}{1+\beta^2\cos^2\psi} \right\} \frac{2\beta\,\mathrm{cosec}\,2\delta \sin\psi\, d\psi}{1+\beta^2\cos^2\psi} . \tag{25}$$

The integrals in this expression are all elementary, except those involving the logarithmic function, and these are evaluated in Appendix I. The final expression obtained is:

$$\frac{C_D}{K^3} = \frac{\pi(1+\beta^2)^3}{4\beta^2}\left(\frac{1+\beta^2}{\beta^2}\log(1+\beta^2) - \frac{1-\beta^2}{1+\beta^2}\right) - \frac{\pi}{8}(1-\beta^2)(5+3\beta^2)$$

$$- \pi\beta\frac{\alpha}{K}\frac{5+3\beta^2}{2} + \pi\left(\frac{\alpha}{K}\right)^2\left(1+\frac{\beta^2}{2}\right) . \tag{26}$$

3. *Results.* Before discussing in detail the results obtained, we must return to the question, raised in Section 1, of the validity of the procedure. The orders of magnitude of the perturbation velocities can be found by inspection.

From equations (15) and (5) we see at once that

$$\frac{v - iw}{U} = \frac{1}{U}\frac{dW}{dZ} = f_1\left(\frac{Z}{s}, \beta\right)\sin\alpha + f_2\left(\frac{Z}{s}, \beta\right)K\beta\cos\alpha$$

and from (17), (14), (15) and (5), by a more careful examination, that

$$\frac{u}{U} = \frac{1}{U}\frac{\partial\phi}{\partial x} = f_3\left(\frac{Z}{s}, \beta\right)K\sin\alpha + f_4\left(\frac{Z}{s}, \beta\right)K^2\beta\cos\alpha ,$$

where $f_i(Z/s, \beta)$ is a function of Z/s and β only, finite for $0 \leqslant \beta \leqslant 1$ in the finite part of the Z plane, except possibly at $Z = \pm s$. Provided $K^2 \ll 1$, i.e., the wing is geometrically slender, even if β is of order unity, equation (19) shows that $\alpha^2 \ll 1$ for the incidences near $\alpha = \alpha_0$ which we chiefly consider. Hence $u \ll U$ and $v^2 + w^2 \ll U^2$ almost everywhere. In particular, if $\alpha = \alpha_0$ (equation (20)), $(v^2 + w^2)/(K^2 U^2)$ and $u/(K^2 U)$ are uniformly bounded in any finite region of the Z plane for $0 \leqslant \beta \leqslant 1$. Thus the results obtained for the perturbation velocities are consistent with the assumptions made about them when the differential equation was linearized, and when equation (16) was written for the pressure coefficient. On the other hand Figs. 4 to 7 show the discrepancies between the treatments using the linearized and the exact boundary conditions, as far as they affect quantities at the incidence α_0. The results of the calculations, therefore, provide as much justification as they can (subject to the reservations in Section 1) for the procedure adopted. (Figs. 4 to 7 are discussed in detail below.)

We now consider the results without restricting the incidence to the neighbourhood of α_0. Thus expressions are obtained which relate to a given wing at different incidences and lift coefficients; it must be remembered that these have only the sort of validity associated with other attached-flow theories of slender wings, when applied through a range of incidence. It should be noted that the expressions for the drag contain a thrust component arising from the singularity in the pressure at the leading edge whenever $\alpha \neq \alpha_0$. No attempt is made here to allow partially for leading-edge separation effects by omitting this component.

The lift coefficient, based on the area of the projection of the wing on the plane $z = 0$, is given

by equation (22). For fixed β, this is linear in α. Numerical values are plotted in Fig. 8 for $\beta = 0$, $0{\cdot}5$ and $1{\cdot}0$. Use of the linearized boundary condition is equivalent to neglecting β^2 compared with unity: the results of doing this are also shown in Fig. 8 for comparison. In a treatment of a wing in which the boundary condition is applied on its surface, it may seem more appropriate to calculate its aspect ratio and force coefficients with reference to its actual or 'developed' area. Using S_d and S_p for this developed area and the area of the wing projection on $z = 0$, we have (*see* Fig. 2):

$$\lambda = \frac{S_d}{S_p} = \frac{2\delta}{\sin 2\delta} = \frac{\delta(1+\beta^2)}{\beta} = 1 + \frac{2}{3}\beta^2 - \frac{2}{15}\beta^4 + 0(\beta^6) \tag{27}$$

$$\left.\begin{aligned} C_{L\,d} &= C_{L\,p}\Big/\lambda \\ C_{D\,d} &= C_{D\,p}\Big/\lambda \\ A_d &= A_p \Big/\lambda \end{aligned}\right\}, \tag{28}$$

where the suffixes d and p have the obvious significance. The coefficient $C_{L\,d}$ based on the developed area is also plotted in Fig. 8 for the three wings. We see that for $\beta = 0{\cdot}5$, the lift coefficient obtained by linearizing the boundary condition (and using the projected area, of course) is only about 4 per cent above that obtained using the exact boundary condition and forming the coefficient from the developed area. Even for $\beta = 1{\cdot}0$, the lift curve slopes, $(1/K)(dC_L/d\alpha)$, based on the exact boundary condition and the developed area and the linearized boundary condition and projected area are within 5 per cent of one another.

The lift-dependent drag coefficient, based on the projected area, is given by equation (26). This is plotted against the incidence in Fig. 9 for the same three values of β as in Fig. 8. Again the curves obtained by using the linearized boundary condition and also by referring the more exact results to the developed wing area are plotted for comparison. The drag coefficients, like the lift coefficients, are remarkably close for $\beta = 0{\cdot}5$. At $\beta = 1$, the discrepancy is much greater, especially near the drag minimum. In both cases the linearized result is closer to the exact result based on the developed area than to that based on the projected area.

Substituting in equation (26), for the drag coefficient, the value of α/K in terms of C_L/K^2 from (22) we have

$$\frac{C_D}{\pi K^3} = \frac{(1+\beta^2)^4}{4\beta^4}\left(\log(1+\beta^2) - \frac{2\beta^2}{2+\beta^2}\right) + \frac{1}{2(2+\beta^2)}\left(\frac{C_L}{\pi K^2}\right)^2. \tag{29}$$

This expression is non-singular for $\beta = 0$, in fact

$$\frac{C_D}{\pi K^3} = \frac{\beta^2}{48}\left(1 + \frac{5}{2}\beta^2 + 0(\beta^4)\right) + \frac{1}{2(2+\beta^2)}\left(\frac{C_L}{\pi K^2}\right)^2. \tag{30}$$

We see, by inspection of (29) and (30), that the minimum lift-dependent drag on a given wing occurs at zero lift, that this minimum increases with the camber and that the familiar relationship for the slender flat plate is recovered for $\beta = 0$. We define the lift-dependent drag factor, κ, in a form independent of the wing area definition:

$$\kappa = \frac{\pi A C_D}{C_L^2} = \frac{4\,C_{D\,p}}{\pi K^3}\Big/\left(\frac{C_{L\,p}}{\pi K^2}\right)^2. \tag{31}$$

Then κ is a decreasing function of C_L for a given wing, bounded below for varying lift by κ_∞, where

$$\kappa > \kappa_\infty = \frac{1}{1 + \frac{1}{2}\beta^2}.$$

The variation of κ with β for fixed C_L is less simple. For each value of C_L, there is a value of β which makes κ a minimum. These values are plotted in Fig. 10 as 'camber needed to attain minimum-drag factor'. For $C_L/\pi K^2 \leqslant 0{\cdot}4$ the required camber is zero*, *i.e.*, the flat plate attains the minimum lift-dependent drag factor for small $C_L/\pi K^2$ on the present theory, as it does for all C_L on the theory with the linearized boundary condition. For larger values of $C_L/\pi K^2$ considerable camber is required to reach the minimum of κ, the optimum wing being half of a circular cone at $C_L/\pi K^2 = 2$. The values of κ obtained by this optimum cambering are also shown in Fig. 10 and we see that a reduction from $\kappa = 1$ for small $C_L/\pi K^2$ to $\kappa = 0{\cdot}773$ at $C_L/\pi K^2 = 2$ takes place.

We now proceed to a more detailed account of the properties of the wing at incidence $\alpha = \alpha_0$, at which incidence the results of the present treatment are expected to approximate most nearly to those for a real fluid, since the type of flow studied is expected to occur. Substituting from (20) in (22) and (26), we find

$$\frac{C_L}{\pi K^2} = \tfrac{1}{2}\beta(1 + \beta^2)^2, \tag{32}$$

$$\frac{C_D}{\pi K^3} = \frac{(1 + \beta^2)^3}{4\beta^2}\left(\frac{1 + \beta^2}{\beta^2}\log(1 + \beta^2) - \frac{1 - \beta^2}{1 + \beta^2}\right) - \frac{(1 - \beta^2)(5 + 3\beta^2)}{8} - \frac{\beta^2(3 + \beta^2)(4 + \beta^2 - \beta^4)}{8}, \tag{33}$$

$$= \frac{\beta^2}{12}\left(1 + \frac{13}{4}\beta^2 + \frac{18}{5}\beta^4 + 0(\beta^6)\right) \tag{34}$$

at the incidence α_0 for which the leading-edge singularity vanishes. The expansion of κ (equation (31)) for small β, at $\alpha = \alpha_0$, is

$$\kappa = \tfrac{4}{3}(1 - \tfrac{3}{4}\beta^2 - \tfrac{3}{5}\beta^4 + 0(\beta^6)). \tag{35}$$

The terms of lowest order in these expansions for small β are the results obtained when the linearized boundary condition is used. Thus $\kappa = 4/3$ is the lift-dependent drag factor calculated in Ref. 9 for the simplest of the slender wings there studied. If we regard the terms of next order as indicating the divergence of the results with the linearized boundary condition from those found here, we are struck by the magnitude of this divergence in the lift and drag coefficients at $\alpha = \alpha_0$. Reference to (20) shows that the linearized estimate of α_0 is not widely out, while (22) and (26) show that, in general, the lift and drag coefficients for given incidence are also close. However, the lift coefficient is given by the difference of two terms which are nearly equal at $\alpha = \alpha_0$ so that small discrepancies in α_0 have disproportionately large effects on C_L, and these affect C_D. To some extent the divergence of C_L and C_D is complementary, so that κ is given more accurately by its linearized value than they are.

---

*For large $C_L/\pi K^2$, the minimum drag occurs where $\partial C_D/\partial\beta = 0$. For small $C_L/\pi K^2$, it occurs at the end point of the permitted range of β^2, i.e., zero.

Fig. 4 shows the incidence, α_0, for no leading edge singularity as a function of the camber, β, for the wings of the family. For $\beta = 0{\cdot}5$ the linearized boundary condition value is less than 8 per cent below the more exact value and only 25 per cent below it at $\beta = 1$. However, in Fig. 5 the effect of this on the lift at this incidence for each wing is shown. The estimate based on the linearized boundary condition is now about 37 per cent in error at $\beta = 0{\cdot}5$ if we compare it with the coefficient based on projected area and about 27 per cent compared with the coefficient based on developed area. Fig. 6 shows that the lift-dependent drag at the incidence at which the singularity is predicted to vanish is already about 50 per cent in error at $\beta = 0{\cdot}5$ if calculated using the linearized boundary condition. The partial cancellation of the errors in lift and drag when the lift-dependent drag factor is calculated is illustrated in Fig. 7. This shows the values of κ at the incidence $\alpha_0 = \alpha_0(\beta)$ for the wings of the family, using the exact and linearized boundary conditions. The latter is constant at $1{\cdot}333$ for all β, but the value based on the exact condition falls from this value at $\beta = 0$, through the minimum for a flat vortex sheet (1) at $\beta = 0{\cdot}67$, to $0{\cdot}773$ at $\beta = 1$. The error in using the linearized boundary condition at $\beta = 0{\cdot}5$ is 18 per cent.

The curves not previously discussed in Fig. 10 are those which relate to wings cambered to eliminate the leading-edge singularity. For a given aspect ratio and lift coefficient, lying within certain ranges, a value of the camber β can be chosen by (32) or Fig. 5 so that a wing with this camber shall have no singularity at the given lift. In this condition the lift-dependent drag factor is obtained from (34) or Fig. 7. The cross-plots so obtained of β and κ as functions of $C_L/\pi K^2$ are shown in Fig. 10 as 'camber needed to eliminate singularity at leading edge' and 'lift-dependent drag factor obtained by cambering for no singularity'. We see that for small values of $C_L/\pi K^2$ there is a considerable difference between the camber for minimum drag factor and the camber for no singularity, while the lift-dependent drag factor with no singularity is well above the minimum. However, the difference rapidly decreases, so that, for $C_L/\pi K^2 = 1$, cambering for no singularity produces a lift-dependent drag only 2 per cent above the minimum for a wing of this family at this lift.

No results have been given for the lift-curve slope, $\partial C_L/\partial\alpha$, at $\alpha = \alpha_0$. It is not certain that this is the same in the two types of flow with separation from all edges and from the trailing edge only. In the partial solutions[13, 14] so far obtained for flat plates with separation from all edges it seems that the lift-curve slopes for the two types of flow agree at the incidence for which both predict trailing-edge separation only, but this is no more than a plausible reason for expecting the same on cambered plates. If the lift-curve slope were the same, it would be given by differentiating (22) with respect to α.

4. *Conclusions.* Thin wings which are geometrically slender and cambered to form portions of circular cones are treated in attached flow by a method more refined than those hitherto available. The boundary condition satisfied by the flow on the wing is applied there instead of on a nearby plane as in the usual linearized theory. From the results we can deduce the following:

(*a*) If the attached flow solution is accepted through the range of incidence, then:

(i) The force coefficients for given camber and leading-edge incidence calculated using the linearized boundary condition are reasonably close to those found using the exact boundary condition. They are, in fact, closer to the exact coefficients if these are based on the developed area of the wing than if they are based on the projected area.

(ii) The lift-dependent drag factor for a given wing decreases with increasing lift, but is bounded below by a function of the camber, which, in turn, decreases as the camber increases.

(iii) The lift-dependent drag factor has a minimum for a fixed lift, which is less than one unless the lift is small. Thus the flat wing is not the most efficient lifting surface of slender triangular plan-form, except, possibly, for small lift coefficients.

(*b*) If we restrict our attention to the results found for the particular incidence on each wing at which the leading-edge singularity vanishes and the attached-flow theory is therefore most trustworthy, then:

(i) This incidence is predicted fairly accurately by the theory with the linearized boundary condition.

(ii) The lift and drag coefficients calculated using the linearized boundary condition at the incidence for no singularity found in the same way are considerably too small. Correspondingly, except for small lift coefficients, the camber required to produce no leading-edge singularity at a given lift is much overestimated by the treatment with the linearized boundary condition.

(iii) The lift-dependent drag factor, though less in error than the lift and drag coefficients, is overestimated for all non-zero values of the camber by using the linearized boundary conditions. Instead of remaining at 4/3 for all cambers it falls from this value for vanishingly small camber to 0·773 for the wing cambered to form half of a circular cone.

(iv) As the lift coefficient increases, the camber designed to eliminate the leading-edge singularity approaches that designed to minimize the lift-dependent drag factor (assuming the attached flow solution applies through the incidence range). The two coincide at $C_L = 2\pi K^2$ (based on projected area), at which lift the half-circular cone has both no leading-edge singularity and the least lift-dependent drag for wings of this type.

It is, unfortunately, not clear how these results should be modified to apply them to other types of camber, in particular to wings whose ordinates are small although their slopes are locally large. In the family studied, large slopes are associated with large ordinates and it is not possible to say whether the slopes alone would produce the same discrepancies between the solutions with different applications of the boundary condition.

LIST OF SYMBOLS

$A = A_p = 4s^2/S_p$	Aspect ratio based on area of projection of wing
$A_d = 4s^2/S_d$	Aspect ratio based on developed area of wing
$C_D = C_{D\,p}$	Drag coefficient based on area of projection of wing
$C_{D\,d}$	Drag coefficient based on developed area of wing
$C_L = C_{L\,p}$	Lift coefficient based on area of projection of wing
C_{Ld}	Lift coefficient based on developed area of wing
C_p	Pressure coefficient
D	Drag
K	Cotangent of leading-edge sweep angle
l	Non-dimensional load distribution
L	Lift
n	Normal to wing surface
s	Wing semi-span
S_d, S_p	Developed and projected areas of wing
U	Undisturbed velocity
u, v, w	Perturbation velocities
W	Complex potential in the cross-flow plane
x, y, z	Rectangular, right-handed co-ordinates, origin at wing apex, Ox downstream, Oy to starboard, with Oxy as the plane containing the leading edges
$Z = y + iz$	Complex co-ordinate in cross-flow plane
Z^*	Complex co-ordinate in circle plane
α	Incidence of undisturbed stream to plane of leading edges
α_0	Value of α for which leading-edge singularity vanishes on a particular wing
β	Camber parameter, ratio of height to semi-span of wing cross-section
$\delta = \tan^{-1}\beta$	One quarter of the angular measure of the wing cross-section
Δ	Difference operator across wing, 'upper − lower'
ζ	Complex co-ordinate in transformed plane
θ	Angular co-ordinate on wing
κ	Lift-dependent drag factor
λ =	S_d/S_p
ρ	Density
ϕ =	$\mathscr{R}\{W\}$, potential in the cross-flow plane
ψ	Co-ordinate on slit in transformed plane.

LIST OF REFERENCES

No.	*Author*	*Title, etc.*
1	O. Laporte and R. C. F. Bartels	An investigation of the exact solutions of the linearized equations for the flow past conical bodies. Bumblebee Series Report 75, John Hopkins University. February, 1948.
2	M. D. Van Dyke	The slender elliptic cone as a model for non-linear supersonic-flow theory. *J. Fluid Mech.* Vol. 1. Part 1. pp. 1 to 15. May, 1956.
3	L. R. Fowell	Exact and approximate solutions for the supersonic delta wing. *J. Ae. Sci.* Vol. 23. Part 8. pp. 709 to 720. August, 1956.
4	L. E. Fraenkel	Supersonic flow past slender bodies of elliptic cross-section. R. & M. 2954. May, 1952.
5	A. Kahane and A. Solarski	Supersonic flow about slender bodies of elliptic cross-sections. *J. Ae. Sci.* Vol. 20. No. 8. p. 513. August, 1953.
6	H. Portnoy	The forces on the general slender body of elliptic cross-section in supersonic flow. *J. Ae. Sci.* (Readers Forum). Vol. 23. No. 1. p. 91. January, 1956.
7	M. A. Heaslet and H. Lomax	Section D of *General Theory of High Speed Aerodynamics.* Ed. W. R. Sears. Oxford University Press. 1955.
8	J. R. Spreiter and A. H. Sacks	A theoretical study of the aerodynamics of slender cruciform wing arrangements and their wakes. N.A.C.A. Tech. Note 3528. March, 1956.
9	J. H. B. Smith and K. W. Mangler	The use of conical camber to produce flow attachment at the leading edge of a delta wing and to minimize lift-dependent drag at sonic and supersonic speeds. R.A.E. Report Aero. 2584. September, 1957.
10	G. G. Brebner	Some simple conical camber shapes to produce low lift-dependent drag on a slender delta wing. R.A.E. Tech. Note Aero. 2529. September, 1957.
11	J. Weber	Design of warped slender wings with the attachment line along the leading edge. R.A.E. Tech. Note Aero. 2530. September, 1957.
12	M. A. Heaslet and J. R. Spreiter	Three-dimensional transonic-flow theory applied to slender wings and bodies. N.A.C.A. Tech. Note 3717. July, 1956.

LIST OF REFERENCES—*continued*

No.	*Author*	*Title, etc.*
13	C. E. Brown and W. H. Michael ..	On slender delta wings with leading edge separation. N.A.C.A. Tech. Note 3430. April, 1955. Published in *J. Ae. Sci.* Vol. 21. No. 10. p. 690. October, 1954.
14	K. W. Mangler and J. H. B. Smith ..	A theory of the flow past a slender delta wing with leading-edge separation. Proc. Roy. Soc. Series A. Vol. 251, pp. 200–217. 26 May, 1959.

Thus by (39) and (40) we find

$$I = \frac{\pi(1+\beta^2)}{2\beta^3}\log\frac{\beta\sqrt{(1-a^2)}+a}{\beta+a\sqrt{(1+\beta^2)}} + \frac{\pi a(1-\beta^2)}{2\beta^2\sqrt{(1+\beta^2)}\{1+\sqrt{(1+\beta^2)}\sqrt{(1-a^2)}\}} \tag{41}$$

or, applying (38), i.e., $a = \sin\delta = \dfrac{\beta}{\sqrt{(1+\beta^2)}}$ and $\sqrt{(1-a^2)} = \dfrac{1}{\sqrt{(1+\beta^2)}}$,

$$I = \frac{1-\beta^2}{4\beta(1+\beta^2)}\pi - \pi\frac{1+\beta^2}{4\beta^3}\log(1+\beta^2)\,. \tag{42}$$

In exactly the same way, we have $\mathcal{J} = \mathcal{J}(a,\beta)$ and

$$\frac{\partial\mathcal{J}}{\partial a} = -2\int_0^{\pi/2}\frac{\sin^2\psi\,(1-\beta^2\cos^2\psi)\,d\psi}{(1-a^2\sin^2\psi)(1+\beta^2\cos^2\psi)^2}$$

$$= -2\left\{\frac{A\pi}{2\sqrt{(1-a^2)}} + \frac{B\pi}{2\sqrt{(1+\beta^2)}} + \frac{C\pi}{4\sqrt{(1+\beta^2)}}\left(1+\frac{1}{1+\beta^2}\right)\right\},$$

where

$$A = \frac{1-\beta^2}{(1+\beta^2)\{a^2(1+\beta^2)-\beta^2\}} + \frac{2\beta^2}{(1+\beta^2)\{a^2(1+\beta^2)-\beta^2\}^2},$$

$$B = \frac{1+\beta^2}{a^2(1+\beta^2)-\beta^2} - \frac{2\beta^2}{\{a^2(1+\beta^2)-\beta^2\}^2},$$

$$C = -\frac{2(1+\beta^2)}{a^2(1+\beta^2)-\beta^2}.$$

Again, $\mathcal{J}(0,\beta) = 0$ and so

$$\mathcal{J} = \frac{-\pi a}{\sqrt{(1+\beta^2)}\{1+\sqrt{(1+\beta^2)}\sqrt{(1-a^2)}\}} \tag{43}$$

or, with $a = \sin\delta$:

$$\mathcal{J} = -\frac{\pi\beta}{2(1+\beta^2)}. \tag{44}$$

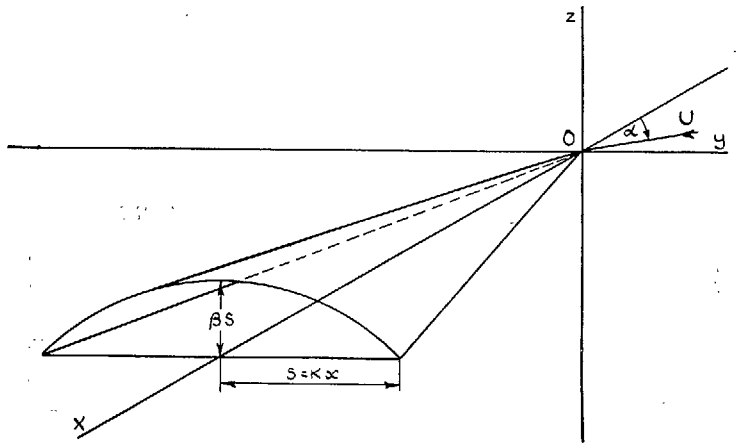

FIG. 1. Co-ordinate system.

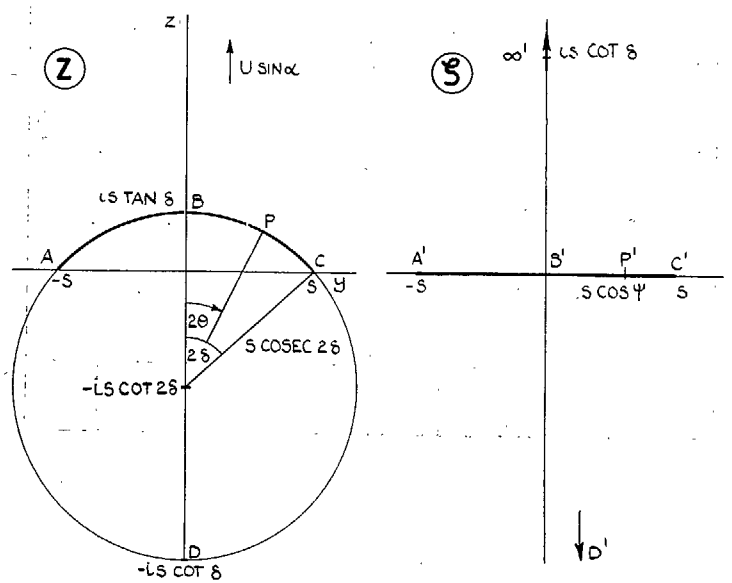

FIG. 2. Cross-flow and transformed planes.

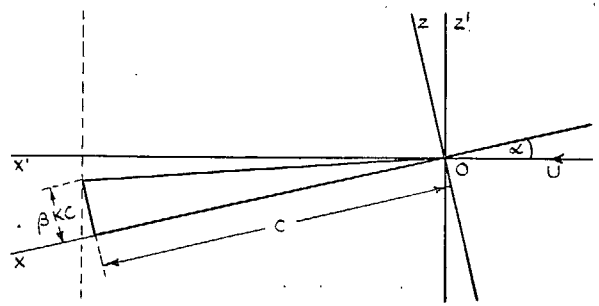

FIG. 3. Control surface for overall forces.

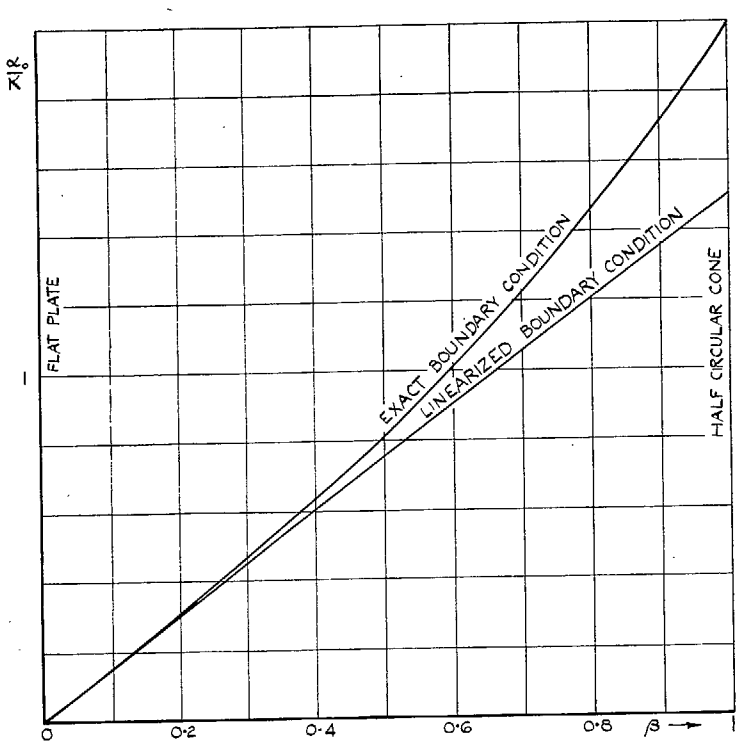

FIG. 4. Incidence for no leading-edge singularity.

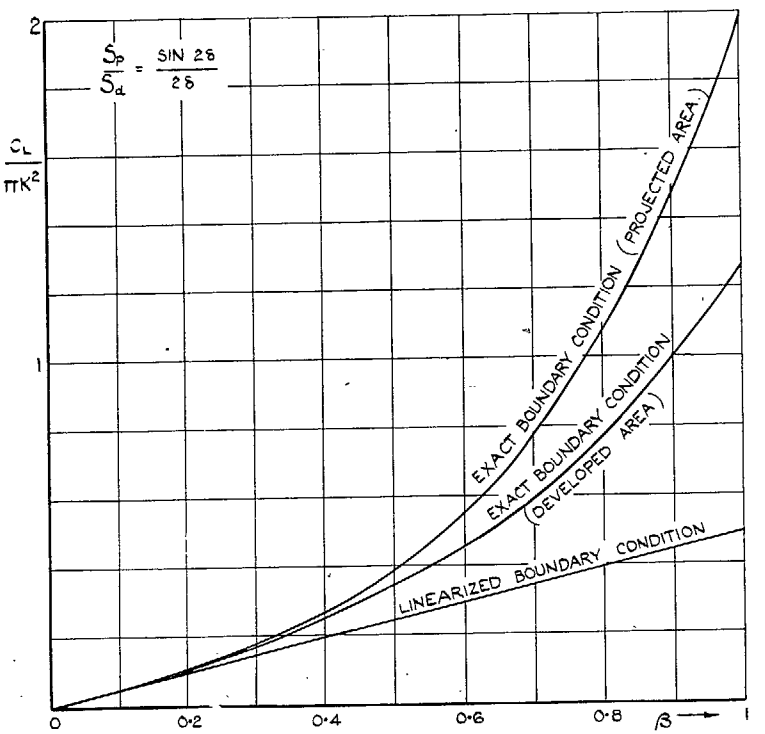

FIG. 5. Lift coefficient at incidence α_0 (No singularity).

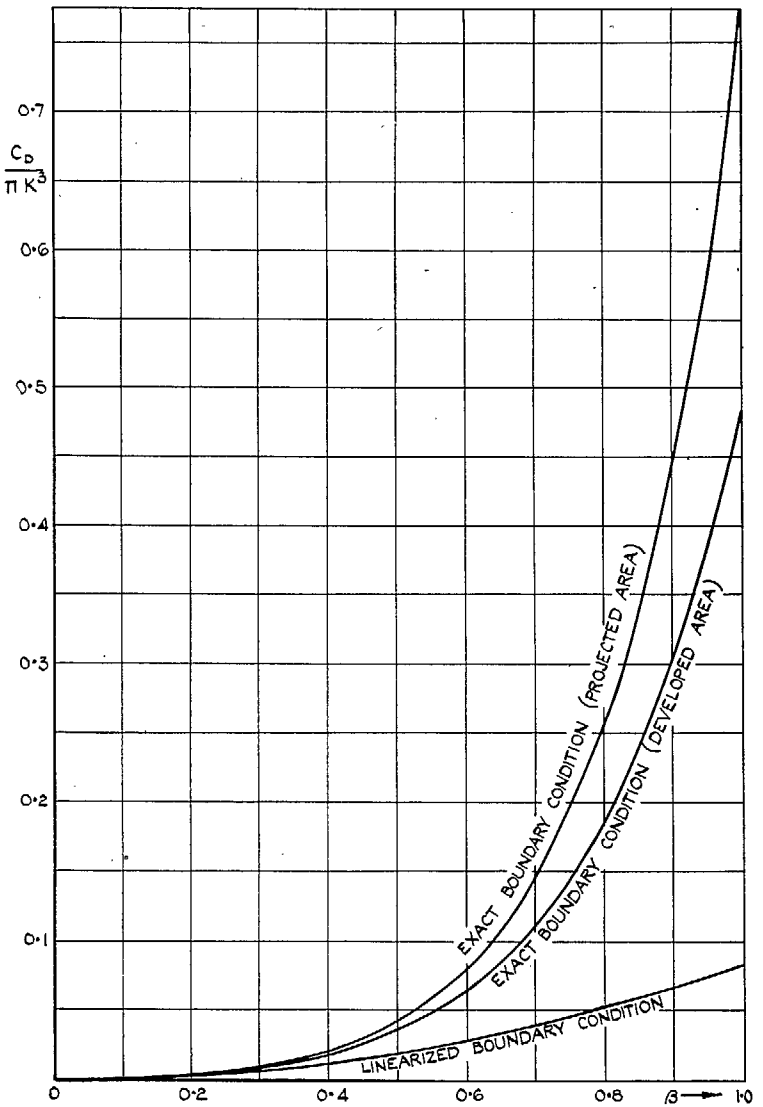

FIG. 6. Lift-dependent drag coefficient at incidence α_0.

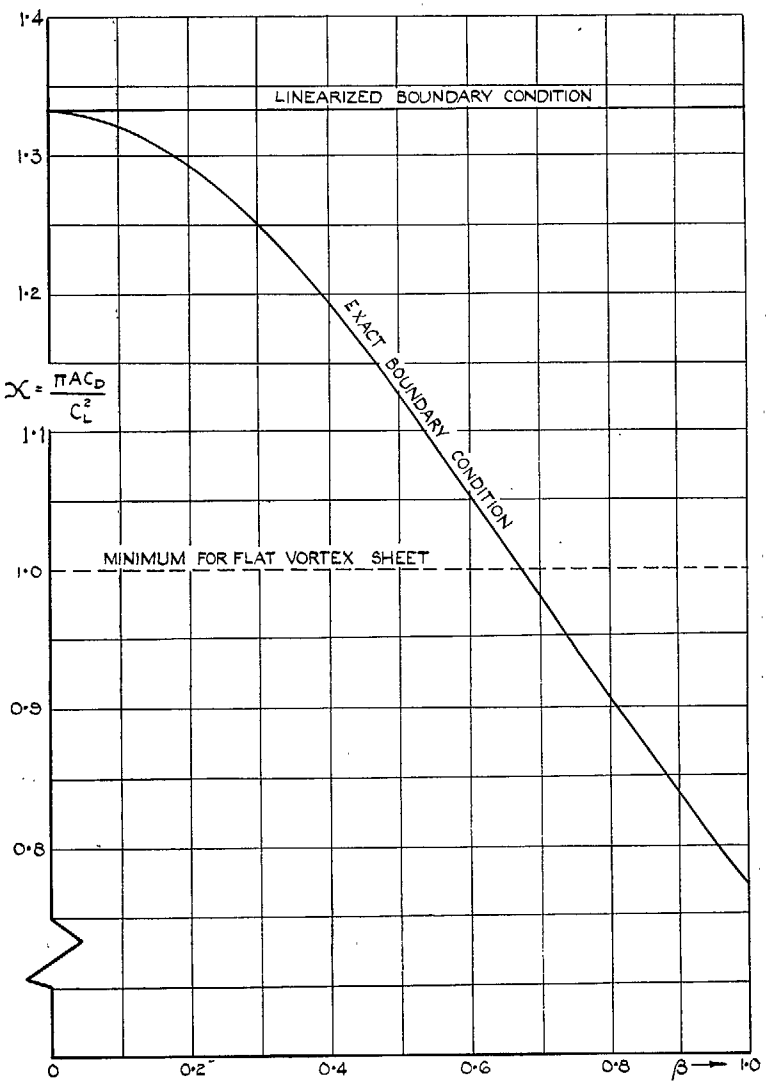

FIG. 7. Lift-dependent drag factor at incidence α_0.

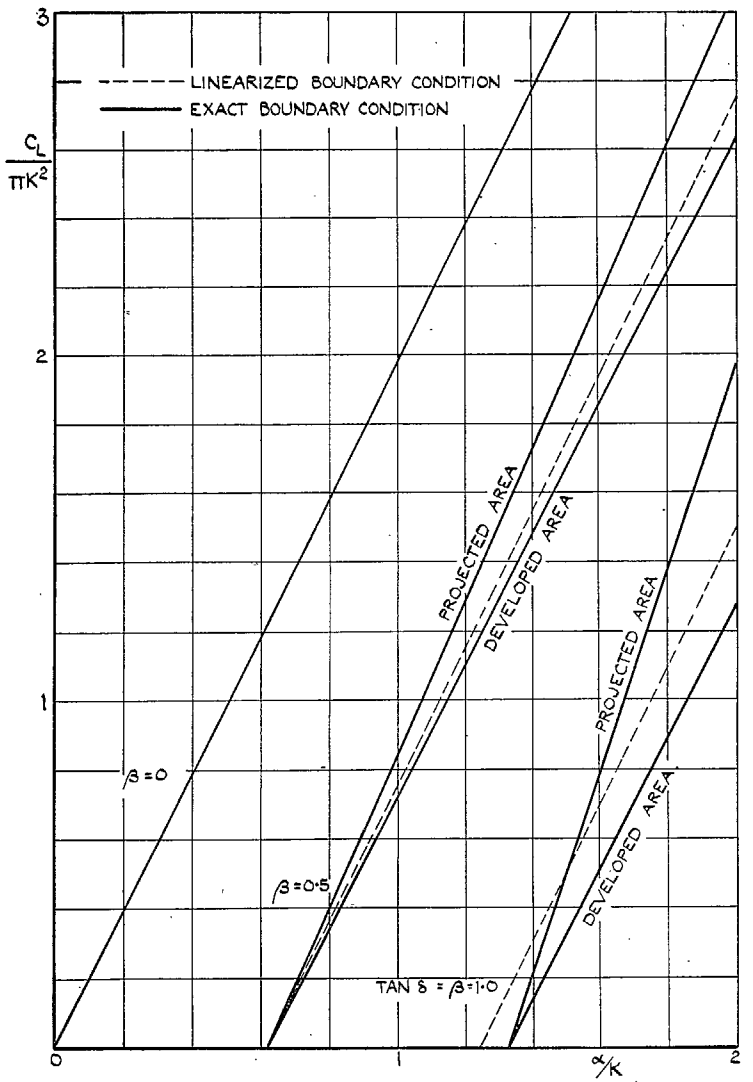

FIG. 8. Lift coefficients of three wings.

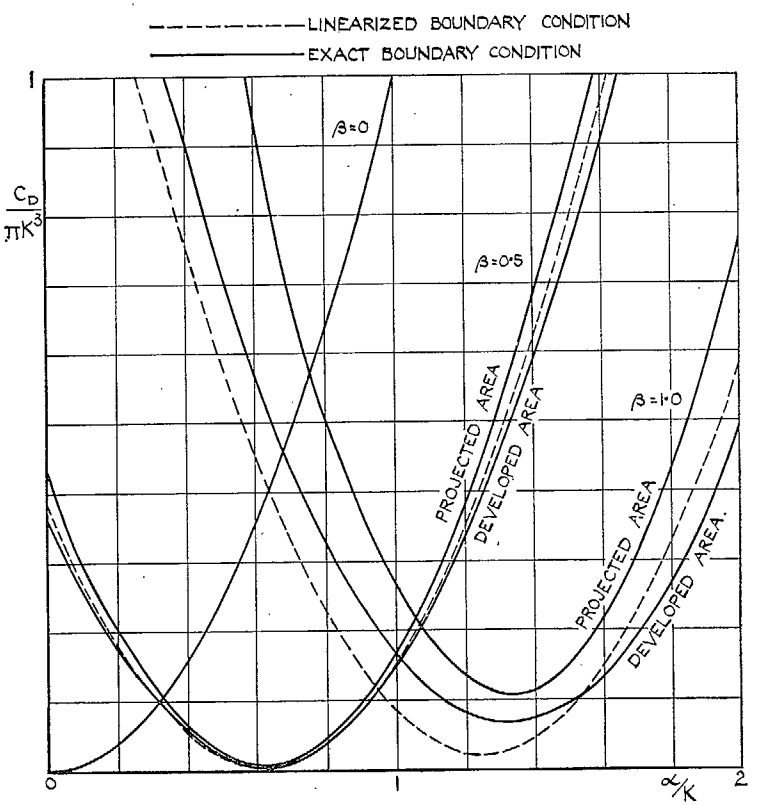

FIG. 9. Drag coefficients of three wings.

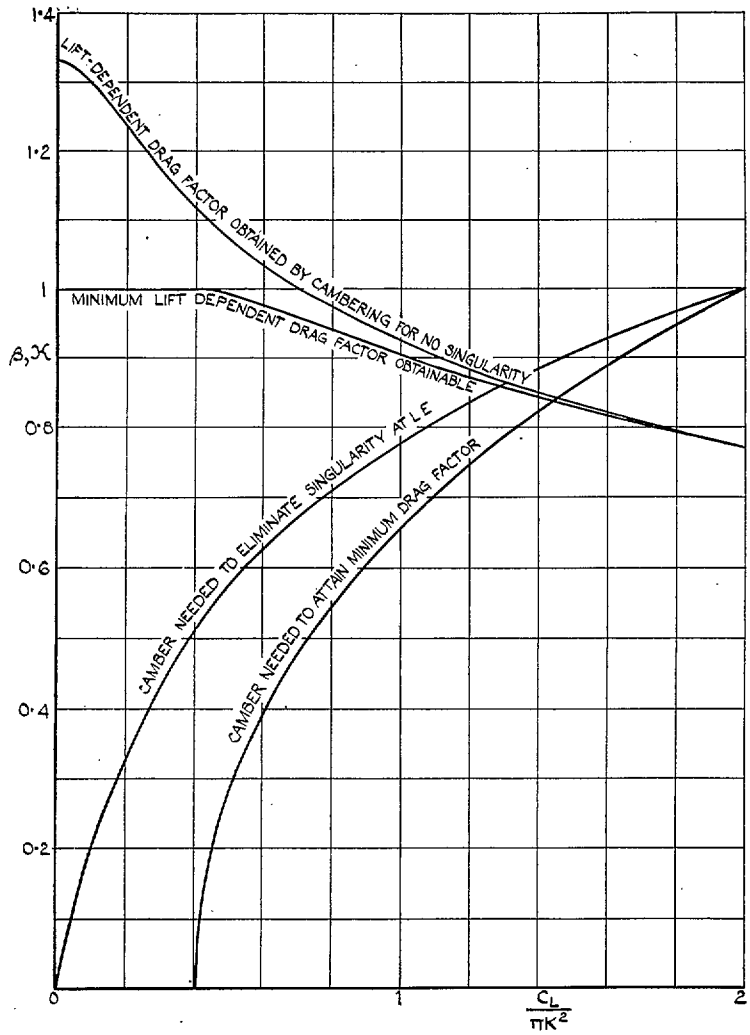

FIG. 10. Camber and drag factor for wings of specified lift coefficient (Based on projected area).

(78801) Wt. 54/8210 K.5 11/60 Hw.

Publications of the Aeronautical Research Council

ANNUAL TECHNICAL REPORTS OF THE AERONAUTICAL RESEARCH COUNCIL (BOUND VOLUMES)

1941 Aero and Hydrodynamics, Aerofoils, Airscrews, Engines, Flutter, Stability and Control, Structures. 63*s.* (post 2*s.* 3*d.*)

1942 Vol. I. Aero and Hydrodynamics, Aerofoils, Airscrews, Engines. 75*s.* (post 2*s.* 3*d.*)
Vol. II. Noise, Parachutes, Stability and Control, Structures, Vibration, Wind Tunnels. 47*s.* 6*d.* (post 1*s.* 9*d.*)

1943 Vol. I. Aerodynamics, Aerofoils, Airscrews. 80*s.* (post 2*s.*)
Vol. II. Engines, Flutter, Materials, Parachutes, Performance, Stability and Control, Structures. 90*s.* (post 2*s.* 3*d.*)

1944 Vol. I. Aero and Hydrodynamics, Aerofoils, Aircraft, Airscrews, Controls. 84*s.* (post 2*s.* 6*d.*)
Vol. II. Flutter and Vibration, Materials, Miscellaneous, Navigation, Parachutes, Performance, Plates and Panels, Stability, Structures, Test Equipment, Wind Tunnels. 84*s.* (post 2*s.* 6*d.*)

1945 Vol. I. Aero and Hydrodynamics, Aerofoils. 130*s.* (post 2*s.* 9*d.*)
Vol. II. Aircraft, Airscrews, Controls. 130*s.* (post 2*s.* 9*d.*)
Vol. III. Flutter and Vibration, Instruments, Miscellaneous, Parachutes, Plates and Panels, Propulsion. 130*s.* (post 2*s.* 6*d.*)
Vol. IV. Stability, Structures, Wind Tunnels, Wind Tunnel Technique. 130*s.* (post 2*s.* 6*d.*)

Special Volumes

Vol. I. Aero and Hydrodynamics, Aerofoils, Controls, Flutter, Kites, Parachutes, Performance, Propulsion, Stability. 126*s.* (post 2*s.* 6*d.*)
Vol. II. Aero and Hydrodynamics, Aerofoils, Airscrews, Controls, Flutter, Materials, Miscellaneous, Parachutes, Propulsion, Stability, Structures. 147*s.* (post 2*s.* 6*d.*)
Vol. III. Aero and Hydrodynamics, Aerofoils, Airscrews, Controls, Flutter, Kites, Miscellaneous, Parachutes, Propulsion, Seaplanes, Stability, Structures, Test Equipment. 189*s.* (post 3*s.* 3*d.*)

Reviews of the Aeronautical Research Council

1939–48 3*s.* (post 5*d.*) 1949–54 5*s.* (post 6*d.*)

Index to all Reports and Memoranda published in the Annual Technical Reports

1909–1947 R. & M. 2600 6*s.* (post 4*d.*)

Author Index to the Reports and Memoranda and Current Papers of the Aeronautical Research Council

February, 1954–February, 1958 R & M. No. 2570 (Revised) (Addendum) 7*s.* 6*d.* (post 4*d.*)

Indexes to the Technical Reports of the Aeronautical Research Council

July 1, 1946–December 31, 1946 R. & M. No. 2150 1*s.* 3*d.* (post 2*d.*)

Published Reports and Memoranda of the Aeronautical Research Council

Between Nos. 2251–2349	R. & M. No. 2350 1*s.* 9*d.* (post 2d.)
Between Nos. 2351–2449	R. & M. No. 2450 2*s.* (post 2*d.*)
Between Nos. 2451–2549	R. & M. No. 2550 2*s.* 6*d.* (post 2*d.*)
Between Nos. 2551–2649	R. & M. No. 2650 2*s.* 6*d.* (post 2*d.*)
Between Nos. 2651–2749	R. & M. No. 2750 2*s.* 6*d.* (post 2*d.*)
Between Nos. 2751–2849	R. & M. No. 2850 2*s.* 6*d.* (post 2*d.*)
Between Nos. 2851–2949	R. & M. No. 2950 3*s.* (post 2*d.*)

HER MAJESTY'S STATIONERY OFFICE

from the addresses overleaf

Printed and published by
HER MAJESTY'S STATIONERY OFFICE

To be purchased from
York House, Kingsway, London W.C.2
423 Oxford Street, London W.1
13A Castle Street, Edinburgh 2
109 St. Mary Street, Cardiff
39 King Street, Manchester 2
50 Fairfax Street, Bristol 1
2 Edmund Street, Birmingham 3
80 Chichester Street, Belfast 1
or through any bookseller

Printed in England

S O. Code No. 23-3135